Astronomy
&
Astrophysics

VLBI astrometry of circumstellar OH masers: Proper motions and parallaxes of four AGB stars

W. H. T. Vlemmings[1,4], H. J. van Langevelde[2], P. J. Diamond[3], H. J. Habing[4], and R. T. Schilizzi[2,4]

[1] Department of Astronomy, Cornell University, Ithaca, NY 14853-6801, USA
[2] Joint Institute for VLBI in Europe, Postbus 2, 7990 AA Dwingeloo, The Netherlands
[3] Jodrell Bank Observatory, University of Manchester, Macclesfield, Cheshire, SK11 9DL, UK
[4] Sterrewacht Leiden, Postbus 9513, 2300 RA Leiden, The Netherlands

Abstract. The main-line OH masers around 4 AGB stars have been observed with the NRAO Very Long Baseline Array (VLBA) at 8 epochs over a period of 2.5 yrs. Using a phase referencing technique, the position of the most compact maser spot of each star was monitored with respect to two extragalactic reference sources. For U Her and W Hya, we observe the most blue-shifted maser spot, while for R Cas and S CrB we only detect a compact red-shifted maser spot. We managed to determine an accurate proper motion and parallax for U Her, R Cas and S CrB, while additional motion of the compact blue-shifted maser of W Hya is shown to possibly be related to the stellar pulsation. The motion and radio position are compared with the stellar trajectory and absolute optical position determined by the Hipparcos satellite. For U Her and W Hya, the most blue-shifted maser is consistent with the amplified stellar image. The new distances are compared with several published $P-L$ relations, and in this respect the VLBI distances seem an improvement upon the Hipparcos distances.

Key words. masers – stars: circumstellar matter – stars: AGB and post-AGB – techniques: interferometric – astrometry

1. Introduction

It was shown in van Langevelde et al. (2000, hereafter vL00) that astrometric observations of the circumstellar OH masers can be used to determine the proper motion and parallax of maser bearing stars. In vL00, observations with the NRAO[1] Very Long Baseline Array (VLBA) were performed on the 1665 and 1667 MHz masers around the Mira variable star U Her. The motion of the masers was traced over 4 yrs and the proper motion and parallax of the underlying star were determined.

In order to use the maser positions to monitor the stellar trajectory, an assumption has to be made about the motion of the masers with respect to the star. In vL00, it was confirmed that, in the case of U Her, the most blue-shifted circumstellar maser spot corresponds to amplified emission originating from the stellar radiophotosphere. The interpretation, in which a high brightness spot in the blue-shifted peak of the OH maser spectrum is expected to mark the line of sight to the star, will be referred to in this paper as the *Amplified Stellar Image Paradigm*. This interpretation was already proposed by

Norris et al. (1984). Very Long Baseline Interferometry (VLBI) observations by Sivagnanam et al. (1990) also provided strong evidence for this, as they showed that in U Her the dominant OH 1665 and 1667 MHz maser features at the blue-shifted side of the maser shell were coinciding, in accordance with the Paradigm. In vL00, the position of the compact blue-shifted maser features was shown to fall directly onto the Hipparcos optical position. MERLIN observations in Vlemmings et al. (2002) indicated that the amplified stellar image of U Her is also seen at the 22 GHz H_2O maser transition.

Maser astrometry yields direct distances to enshrouded stars. This allows the inclusion of the more extreme Mira stars in studies of the fundamental properties of these stars, like the pulsation and mass-loss mechanism. The current discussion on the $P-L$ relation (e.g. Whitelock & Feast 2000), for instance, could then include stars with higher mass loss and generally longer periods. At the moment these investigations are based on Hipparcos distances, which excludes the stars with high mass-loss because they tend to be too obscured in the optical. A similar outstanding debate considers the precise pulsation mode of Mira variables; this requires the conversion of IR interferometry data into absolute diameters and hence distances (van Leeuwen et al. 1997; Wood 1998).

Here we observed an additional 3 stars in the astrometric OH maser monitoring campaign which was also continued on U Her. All four stars were observed with Hipparcos

Send offprint requests to: W. H. T. Vlemmings,
e-mail: wouter@astro.cornell.edu

[1] The National Radio Astronomy Observatory is a facility of the National Science Foundation operated under cooperative agreement by Associated Universities, Inc.

Table 1. The sample.

Source	Period	V_{star}	Hipparcos parallax	Hipparcos Parallax[a]	Hipparcos Proper motion	
	(days)	(km s^{-1})	(mas)	(mas)	RA, Dec (mas/yr)	
W Hya	361	40.0	8.73 ± 1.09	12.85 ± 0.99	−49.05 ± 1.18	−59.58 ± 0.78
S CrB	360	0.0	1.90 ± 1.36	2.40 ± 1.17	−8.33 ± 0.93	−11.55 ± 0.62
U Her	406	14.5	1.64 ± 1.31	1.88 ± 1.31	−16.84 ± 0.82	−9.83 ± 0.92
R Cas	430	26.0	9.37 ± 1.10	10.04 ± 1.10	84.39 ± 0.95	18.07 ± 0.88

[a] Recalculated by Knapp et al. (2003)

Table 2. Sources with corresponding reference sources.

Source	Ref. #	Calibrator	RA (^{h} ^{m} ^{s})	Dec (° ′ ″)	Sep. (°)	Flux (mJy)
W Hya	1	J1339-262	13 39 19.890747	−26 20 30.49590	2.9	515 ± 62
	2	J1342-290	13 42 15.345608	−29 00 41.83114	1.6	162 ± 44
S CrB	1	J1522+3144	15 22 09.991716	31 44 14.38214	0.4	362 ± 79
	2	J1527+3115	15 27 18.73703	31 15 24.38625	1.3	151 ± 15
U Her	1	J1636+2112	16 36 38.18373	21 12 55.5991	3.5	217 ± 30
	2	J1630+2131	16 30 11.23117	21 31 34.3144	2.8	92 ± 12
R Cas	1	J2355+495	23 55 09.458179	49 50 08.34000	1.6	832 ± 70
	2	J2347+5142	23 47 04.83800	51 42 17.87700	1.8	72 ± 12

(Perryman et al. 1997) and the Hipparcos parallaxes were recently recalculated by Knapp et al. (2003). However, because our target stars are faint and variable, the Hipparcos results, especially on the parallax, are quite uncertain. Our VLBI results improve upon the Hipparcos results. They also further provide statistics on the *Amplified Stellar Image Paradigm*, confirming the results on U Her and W Hya, while R Cas and S CrB surprisingly show only a compact red-shifted maser spot that nonetheless could be traced for over two years.

In Sect. 2 we discuss the observations and the absolute astrometry and error analysis. In Sect. 3 we give the results of our parallax and proper motion determination, which we discuss in Sect. 4. The conclusions are presented in Sect. 5.

2. Observations

The positions of the 1665 and 1667 MHz circumstellar OH masers of a sample of 4 AGB stars were monitored over a period of almost 2.5 yrs with the NRAO VLBA. The sample of stars consisted of the Mira variable stars R Cas, S CrB, U Her and the Semi-Regular star W Hya. The observations were performed over 9 epochs. These are October 9, 1999, January 20, 2000, June 7, 2000, September 1, 2000, December 15, 2000, March 11, 2001, May 27, 2001, February 23, 2002 and May 12, 2002. The observations of March 11, 2000 failed due to heightened ionospheric activity caused by the solar maximum. The OH masers around U Her were already previously monitored between July 1994 and April 1998 and the results of those observations are presented in vL00.

The sources were selected to have bright 1665 and/or 1667 MHz OH masers. Also, the sources were chosen so that two bright nearby phase reference sources were available. Finally, the stars were selected to be within ≈500 pc in order to have detectable parallaxes of more than ∼2 mas. The stars in our sample with their period, stellar velocity with respect to

the Local Standard of Rest (LSR) and Hipparcos proper motion and parallax are given in Table 1.

For each epoch the total observation time was 12 hrs. During the first 2 epochs 4 additional stars were observed (R Crt, RT Vir, RS Vir and R Aql). Both RS Vir and R Aql were observed at the 1612 MHz instead of the 1665 MHz transition. R Crt was not detected and we were unable to get a phase connection to the phase reference sources of RT Vir, RS Vir and R Aql. We also found that in 12 hrs we can obtain only sufficient uv-coverage for 4 sources, because the beam-shape is important to measure accurate positions. For U Her, S CrB and R Cas this resulted in an average beam size of 12 × 7 mas. Because of a low declination, the beam for W Hya is strongly elongated and is on average 20 × 8 mas.

In every star both the maser lines were observed in dual polarization, with a bandwidth of 500 kHz centered on the stellar velocity. They were correlated with moderate spectral resolution (1.95 kHz = 0.36 km s^{-1}). Simultaneously two 4 MHz wide bands were recorded to detect the continuum reference sources. These were correlated with a spectral resolution of 31.7 kHz for the final two epochs and 125 kHz on the others.

The extragalactic reference sources were selected from the VLBI calibrator catalogue (Beasley et al. 2002). The positions of the reference sources for U Her, J1636+2112 and J1630+2131 (formerly J1628+214), were refined in vL00. In Table 2 we list the observed sources with their reference sources, and the separation between the star and the reference source. Our phase reference cycle was 5 min, with 3 min per source and then 1 min for each of the calibrators. The calibrator positions with respect to the source position are plotted in Fig. 1.

The data was then processed in AIPS without any special astrometric software. We rely on the VLBA correlator model and work with the residual phases directly. To be able to apply the phase, delay and phase rate solutions obtained on the
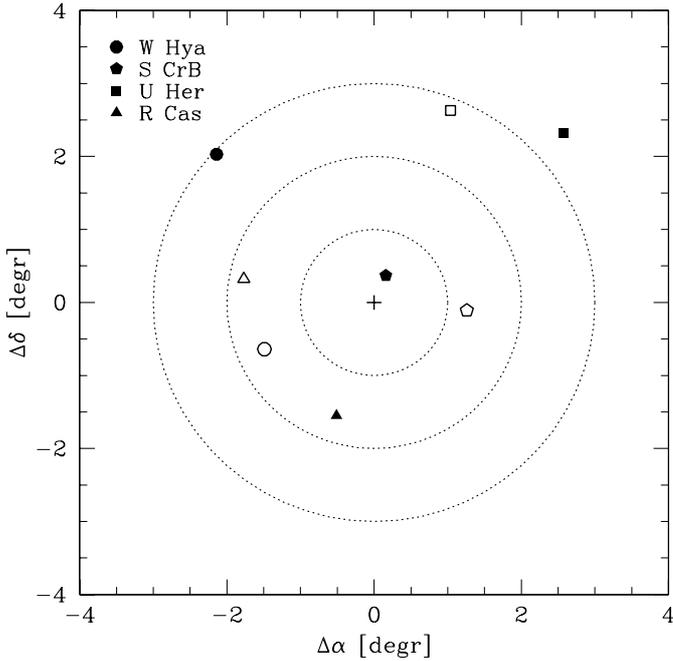
Fig. 1. Reference source positions wrt the target star in Right Ascension and Declination off-set. The sources are indicated with the listed symbols where the solid symbols are reference source 1, and the open symbols reference source 2. The circles are plotted to guide the eye and have a diameter of 2, 4 and 6 degrees.
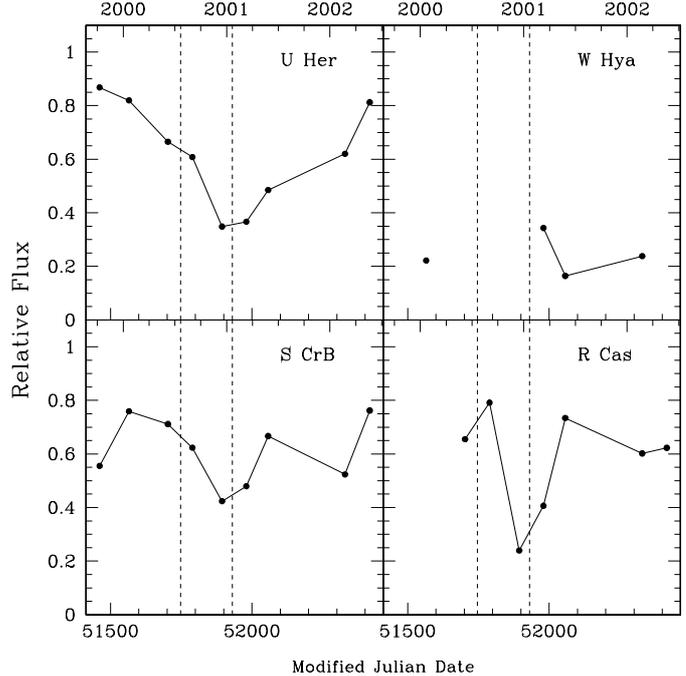

Fig. 2. The ratio between the flux density of reference source 1 when phase-referenced to reference source 2 and the flux density when using the phase, delay and phase rate solutions obtained on reference source 1 itself. The dashed vertical lines indicates the approximate period maximum solar activity.

continuum reference sources, a special task was written to connect the calibration of the wide band data to the spectral line data.

2.1. Ionospheric effects

The correlator model does not include an ionospheric model. Phase referencing will approximate the ionospheric conditions by zero order in position and first order in time. For our analysis no additional ionospheric modeling is included. As noted in vL00, the remaining effects of ionospheric activity can be seen as slightly distorted images

Unfortunately, the observations were performed during the period of solar maximum, which occurred in the last months of 2000. Due to this maximum in solar activity the ionosphere affects the phase referencing, which is illustrated in Fig. 2. Here we display the ratio between the flux density of one of the reference sources when it is imaged directly and the flux density when it is imaged with the calibration solution on the second reference source. While for the reference sources of W Hya the sources were too far apart to obtain good phase connection for most of the epochs, we notice that on the other three pairs of reference sources a significant amount of coherence on these scales is lost due to ionospheric activity. Furthermore, we also find that the phase connections are slightly worse during daytime. Thus, as a result of the heightened ionospheric activity, the positional accuracy will be less.

2.2. Absolute astrometry

The absolute astrometry of the maser spots was determined with respect to the two extragalactic reference sources. As a consistency check we also determined the positions of the reference sources with respect to each other. The results for the reference sources of U Her are shown in Fig. 3, and the results for those of S CrB and R Cas in Fig. 4. As was already seen in Fig. 2, no accurate phase connection was established between the reference sources of W Hya. We find that the reference sources J1630+1231 (of U Her) and J2355+495 (of R Cas) show relatively large extended structure on the VLBA baselines. J1630+1231 has some indication of a single jet structure, while J2355+495 clearly shows two radio lobes. For the first epoch of U Her a detailed source model was used for the phase referencing, but this seemed to have little effect. For the epochs presented here a point source model was used and the effect on the astrometric positions is shown in Figs. 3 and 4. When examining the separation between the reference sources of U Her, we notice that source evolution might cause a slight drift in the obtained relative positions. A linear fit to this motion indicates that the astrometric positions with respect to J1630+1231 show a drift of ≈0.57 and 0.10 mas/yr in right ascension and declination respectively. This would influence the derived proper motions by a similar amount, and it explains some of the discrepancy between the Hipparcos and VLBI proper motions. The determined parallax will not be affected as no periodic motions correlated between right ascension and declination seem to be present. The double lobe structure of J2355+495 does not seem to cause any systematic effect, although the scatter on the
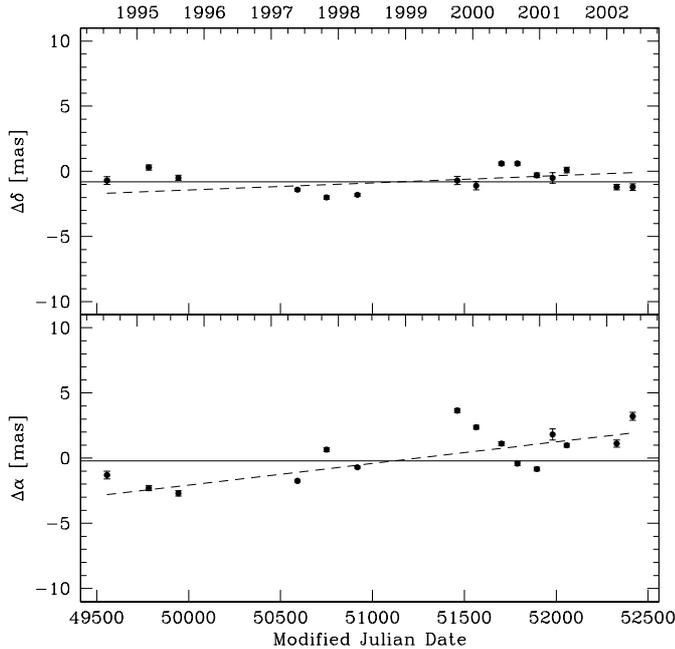
Fig. 3. The difference between the measured separation and its a priori value of U Her reference source 1 (J1636+2112) with respect to 2 (J1630+2131, formerly J1628+214). The solid line indicates the average separation between the reference sources. The dashed line is a weighted least square fit to a change in measured separation due to evolving source structure of J1630+2131.

Fig. 4. The difference between the measured separation and its a priori value of S CrB reference source 1 (J1522+3144) with respect to 2 (J1527+3115), and R Cas reference source 2 (J2347+5142) with respect to 1 (J2355+495). The formal error bars lie within the plotted symbols. The solid line indicates the average separation between the reference sources and the dashed lines are the rms.

position determination is slightly bigger. However, this is likely also due to the fact that the scatter in the difference between measured and a priori assumed separation increases with increasing source separation.

2.3. Error analysis

There are several sources of errors in the determination of our astrometric positions. One of these is the influence of the ionosphere. As discussed above, the phase referencing will solve for the zeroth order effect. The errors as a result of the phase referencing over the ionosphere between the reference source and the maser source are estimated by examining the difference between the measured separation between the reference sources and their a priori expected separation as shown in Figs. 3 and 4. From this we first determine the average offset of the reference sources with respect to the expected positions; this error is due to the error in the *absolute* position of the reference sources. Then we determine the scatter, which can be attributed to the phase referencing. For R Cas we find that the difference between the measured separation and its a priori value is 5.1 ± 3.6 mas. For S CrB we find 1.1 ± 2.5 mas. If for U Her, we simply take the average offset we find 0.71 ± 1.5 mas. When using the least-square fitted line discussed in the previous section the scatter decreases to 1.1 mas. Unfortunately, no error analysis could be performed for W Hya, and we take the errors to be similar as for R Cas.

Depending on the position of the target source with respect to the reference sources, we generally find the largest scatter along the declination axis. As the depth of the ionosphere along
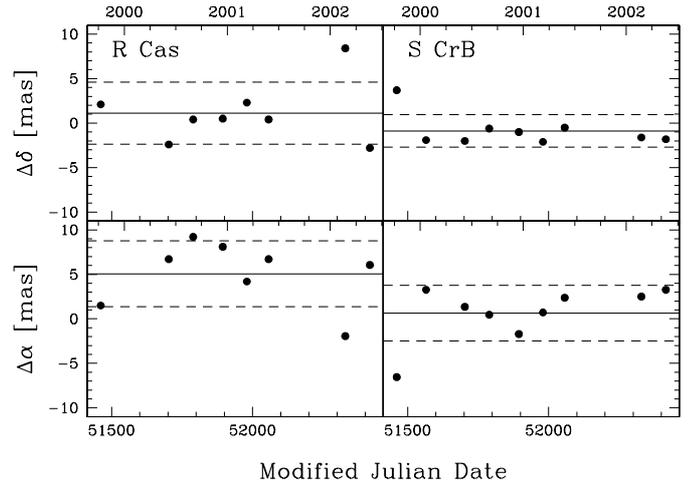
the line of sight changes faster with a change in declination than with a change in right ascension, the ionospheric errors in right ascension are less than those in declination for a separation which is comparable in each coordinate.

According to the VLBA calibrator list, the positions of all the reference sources, except for J2347+5142 (from R Cas) and J1630+2131 (from U Her), are known within 1 mas accuracy. In vL00 we have observed J1630+2131 ourselves, and the positions used here are also accurate within 1 mas. The position of J2347+5142 is still only known to within 20 mas. Thus, the average positional offset for the reference sources of U Her and S CrB agrees well with the estimated accuracy of ≈ 2 mas for the *absolute* positions of the reference sources. The average offset for the calibrators of R Cas is larger, which was expected as the J2347+5142 positions are less accurately known.

Errors also arise from the formal positional fitting. The fitting was performed with the routine JMFIT in AIPS, where we fitted the 6 components of a Gaussian feature (position, long and short axis, position angle and peak flux). The formal errors depend on the beam size and the thermal fluctuation in the mapped spectral channel where the maser feature occurs. The errors are approximately proportional to Beamsize/SNR. This is generally less than 1 mas for most of our observations, although, since the signal-to-noise ratio (SNR) is also affected by the ionosphere, the error could reach ≈ 3 mas in each coordinate for W Hya and $\approx 1-1.5$ mas for the other sources. As most of our maser features are resolved, higher resolution will not increase the positional accuracy.

3. Results

3.1. Morphology

Of our sources, only U Her shows multiple blue and red-shifted features on VLBA baselines. We only managed to identify one bright maser feature for S CrB, W Hya and R Cas. We were
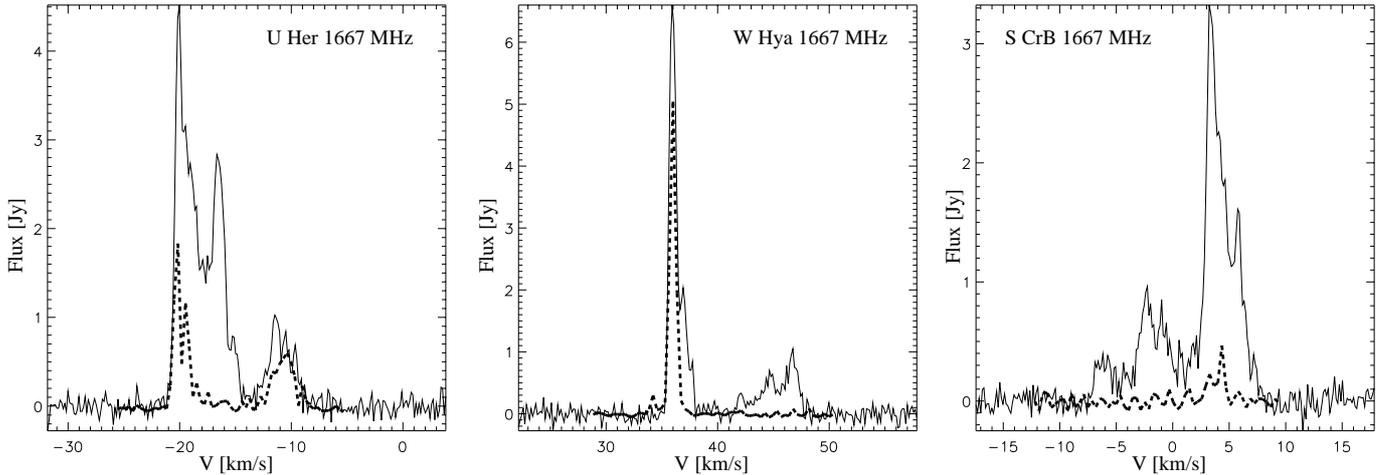
Fig. 5. The 1667 MHz maser spectra of U Her, W Hya and S CrB. The solid line is the single dish spectrum in left-hand circular polarization for U Her and S CrB and right-hand circular polarization for W Hya. The spectra are from Etoka & Le Squeren (2000) and Etoka et al. (2001), and were taken in 1984 (U Her) and 1986 (W Hya and S CrB) at the Nancay radio telescope. The thick dashed line is the maser spectrum at a short VLBA baseline (Pt-La) from the last observing epoch (May 12, 2002).

able to image both 1665 and 1667 MHz masers in U Her, W Hya and S CrB, while for R Cas only the 1665 MHz maser was bright enough.

Figure 5 shows the 1667 spectrum of U Her on one of the short VLBA baselines compared with the single dish spectrum. We see that the features span a range between -8 and -21 km s^{-1} around the stellar velocity of -14.5 km s^{-1}. Due to the ionospheric activity the double peaked spectrum was only observed in the epochs presented in vL00, and in the last two epochs. For the other epochs we could only map the most blue-shifted feature. Thus, we did not include other maser spots in our astrometric analysis. At the 1665 MHz transition, the most blue shifted spot is found slightly shifted in velocity with respect to the 1667 MHz most blue-shifted feature. The most blue-shifted 1665 feature has a velocity of -20.8 km s^{-1}, while the most blue-shifted 1667 feature has a velocity of -20.4 km s^{-1}. Similarly as in vL00, we find that in most cases the bright 1665 and 1667 maser features coincide within the synthesized beam. Since at the epochs in vL00 we only used the most blue-shifted 1667 maser spot to determine the proper motions and parallax, here we also only use the 1667 spot.

In W Hya we only detected one bright maser spot at 35.6 km s^{-1} in both maser transitions. Figure 5 shows a short VLBA baseline 1667 spectrum compared with the single dish spectrum. The positions of the 1665 and 1667 maser spots coincide within the beam, which, since W Hya is observed at very low declination, is highly elongated along the declination axis. The bright feature we detected corresponds in velocity to the brightest maser feature detected by Szymczak et al. (1998). This is the most blue-shifted feature at 1665 MHz, whereas at 1667 MHz a more blue-shifted, slightly weaker feature is found at 33.9 km s^{-1}. This weaker feature was only detected at our last epoch and is found to exist at $\approx$17.2 mas from the brightest feature.

Around S CrB we detected only one bright maser feature at both transitions, which is red-shifted with respect to the stellar velocity of 0.0 km s^{-1}. The feature at 1665 MHz is found to coincide within the beam with the 1667 MHz spot, although the velocity at 1667 MHz is 3.2 km s^{-1} and the velocity at 1665 MHz is 2.9 km s^{-1}. We find that these features correspond to the brightest features in the single dish spectra presented by Etoka & Le Squeren (2000) and the spectrum seen in Fig. 5, which is not necessarily the most red-shifted. Also in the single dish spectra, the main-line masers show only weak blue-shifted emission, while the 1612 MHz satellite line shows a strong blue-shifted peak.

Finally, around R Cas we only detected a narrow maser feature at 1665 MHz, at a velocity of 29.5 km s^{-1}. This is red-shifted with respect to the stellar velocity of 26.5 km s^{-1}. In the single dish spectrum observed by Chapman et al. (1994), the brightest feature is found red-shifted as well, at a velocity of 29.2 km s^{-1}. However, this was not the most red-shifted feature, as still weaker features were found at higher velocity.

3.2. Proper motion/parallax

The proper motion and parallax for our sample of sources were determined using a least-square fitting method. For U Her we included the data of the 6 epochs presented earlier in vL00. When the spot was observed in both transitions (for W Hya and S CrB), we performed the fit on both the spots separately as well as on the combined data. The errors due to the thermal fluctuation are not correlated for the two frequencies, but the systematic ionospheric effects can be. The results of the fits are presented in Table 3 along with the number of epochs at which the maser feature was detected. The errors represent the 1σ deviations. In the further analysis for W Hya and S CrB, we take the fit to the combined 1665 and 1667 data as the most reliable estimate.

The fitted motions and observed positions are presented in Figs. 6–9. The errors displayed are the formal uncertainties in the Gaussian profile fitting used to determine the positions. As discussed above these were less than 1 mas at most epochs,
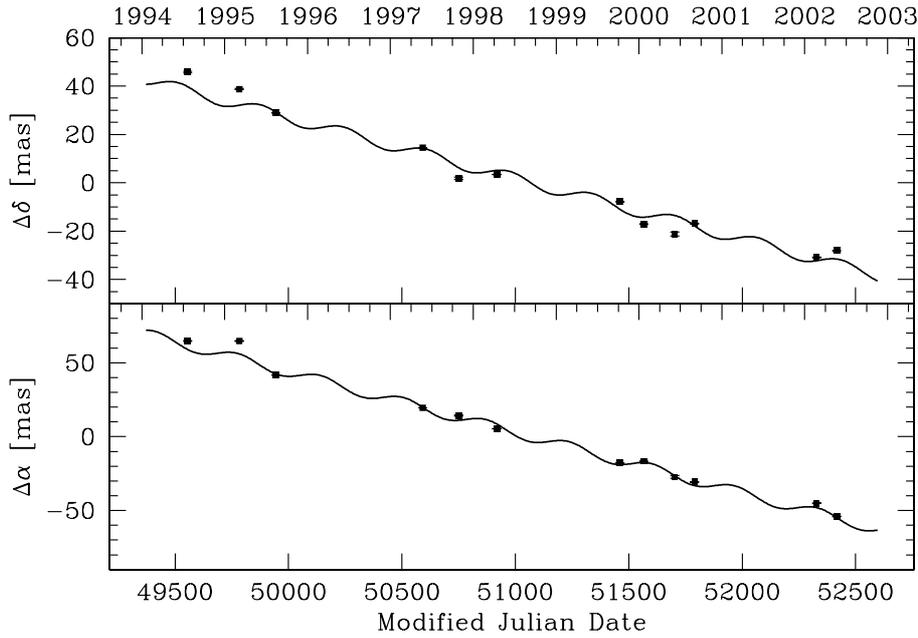
Fig. 6. The position of the most blue-shifted 1667 MHz maser spot of U Her with respect to J1630+2131. The error bars on the positions indicate the formal position fitting errors. The solid line is the best fitting parallax and proper motion trajectory for the 12 epochs of observations. Note that the scales are different for declination and right ascension.
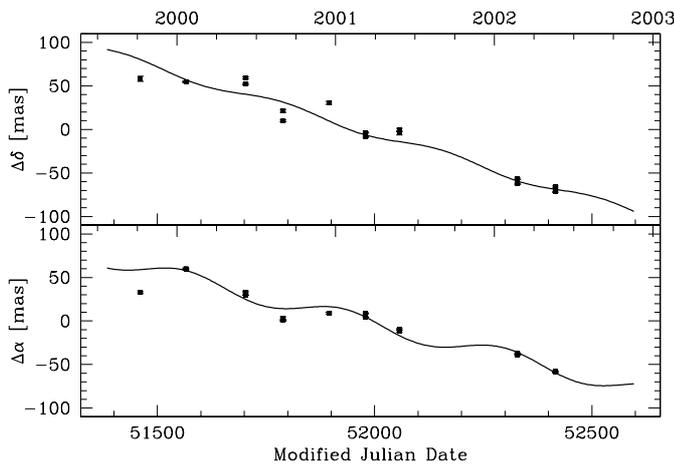

Fig. 7. Similar to Fig. 6. The position of the most blue-shifted 1665 and 1667 MHz maser spots of W Hya with respect to J1342-290. The 1665 and 1667 maser spots have the same velocity. Drawn is the best fitting parallax and proper motion trajectory combining the results on both maser transitions for the 8 epochs of observations.

Fig. 8. Similar to Fig. 6. The position of the brightest 1665 and 1667 MHz maser spots of S CrB with respect to J1522+3144. The brightest S CrB maser feature is red-shifted with respect to the stellar velocity. The 1665 and 1667 maser spots have the same velocity. Drawn is the best fitting parallax and proper motion trajectory combining the results on both maser transitions for the 8 epochs of observations.
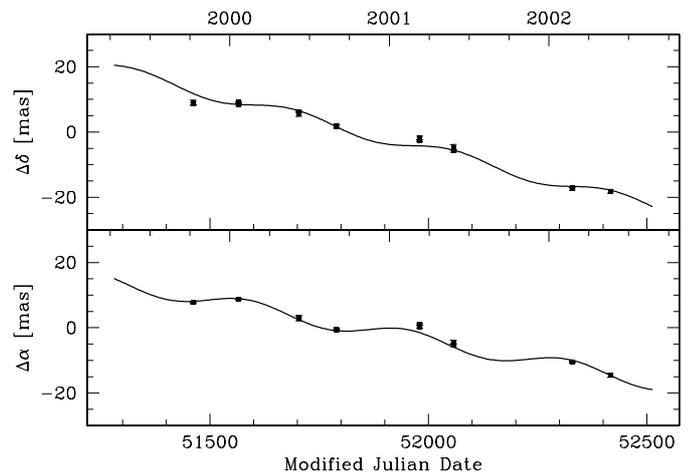
but could go up to ≈1.5 mas (or even 3.0 mas in the case of W Hya) as the ionospheric conditions worsened.

As previously seen in vL00, the final fit for U Her leaves rms residuals somewhat larger than those estimated to be caused by the phase referencing. These cannot be caused by the possible linear drift of the reference source position, as this will only change the measured proper motion. We find weighted rms residuals of 3.0 and 3.1 mas in right ascension and declination respectively, while from the reference sources we expected residuals of ≈1.5 mas. It should be noted however, that the separation between U Her and its reference source is bigger than the separation between the reference sources themselves, and this we think is the cause of the larger residuals. The separation between U Her and its reference source is 2.8°, similar to the

separation between the R Cas reference sources. Thus residuals of ≈3 mas can be expected.

For S CrB we find weighted rms residuals of only 1.0 and 1.3 mas in right ascension and declination. This agrees very well with the systematic errors in the relative astrometry originating from the ionospheric activity, which were estimated to be ≈2.5 mas. The residuals are smaller likely due to the fact that the source-reference source separation is less than between the reference sources. The weighted rms residuals for R Cas are somewhat larger (2.2 and 4.6 mas), but, when the position fitting errors are taken into account, they still agree with the expected value of 3.6 mas. Finally, the weighted rms residuals for W Hya are quite large (7.8 and 10.2 mas). Although we

Table 3. Results.

Source	MHz	VLBI parallax	VLBI Proper motion		# epochs
		(mas)	RA, Dec (mas/yr)		
W Hya	1665	9.79 ± 3.23	-45.54 ± 3.02	-53.82 ± 5.08	8
	1667	12.50 ± 4.23	-41.80 ± 3.14	-56.39 ± 3.65	8
	both	10.18 ± 2.36	-44.24 ± 2.04	-55.28 ± 2.93	
S CrB	1665	2.37 ± 0.43	-8.92 ± 0.38	-12.21 ± 0.65	7
	1667	2.30 ± 0.50	-9.13 ± 0.41	-12.53 ± 0.46	8
	both	2.31 ± 0.33	-9.08 ± 0.27	-12.49 ± 0.33	
U Her	1667	3.61 ± 1.04	-14.94 ± 0.38	-9.17 ± 0.42	12
R Cas	1665	5.67 ± 1.95	80.52 ± 2.35	17.10 ± 1.75	8
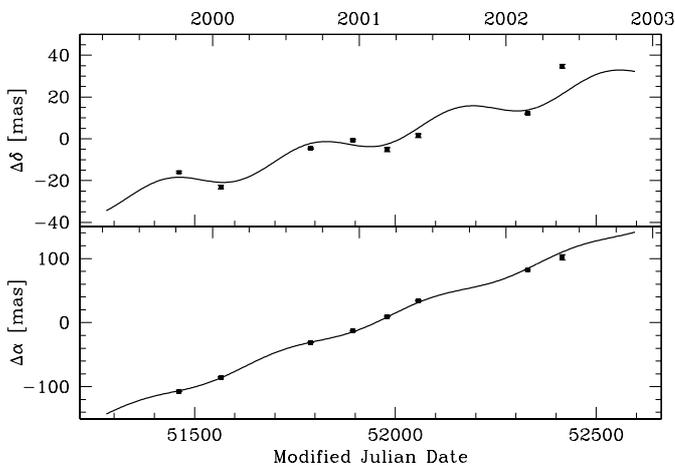
Fig. 9. Similar to Fig. 6. The position of the brightest 1665 MHz maser spot of R Cas with respect to J2355+495. The brightest R Cas maser feature is red-shifted with respect to the stellar velocity. Drawn is the best fitting parallax and proper motion trajectory combining the results on both maser transitions for the 8 epochs of observations.

Table 4. Hipparcos flags.

Source	H29	H30	H59	H61
	(%)			
W Hya	4	5.15	V	
S CrB	2	2.31	V	
U Her	0	2.24		S
R Cas	0	2.53	V	

were unable to examine the ionospheric effects on the reference sources, these residuals are too large to be caused only by ionospheric effects. The maser spots seem to show some additional systematic periodic motion, which is discussed in Sect. 4.1.2.

For both U Her and W Hya, where the most blue-shifted maser spot is expected to be the amplified stellar image, we have also performed a fit including the Hipparcos optical positions as an additional data point. From the Hipparcos catalogue we take the positional uncertainty to be 0.1 mas. The fit on U Her then resulted in $\mu = -14.86 \pm 0.25$, -9.50 ± 0.27 mas/yr and $\pi = 3.34 \pm 0.90$. The fit on W Hya gave $\mu = -51.69 \pm 0.28$, -62.00 ± 0.46 mas/yr and $\pi = 9.65 \pm 3.00$ mas. However, one should realize that using the Hipparcos position as an additional data point encompasses one more uncertainty, namely the connection between the optical and radio reference frames, which in principal introduces additional systematic errors.

3.3. Hipparcos comparison

By comparing Table 3 with Table 1, we find that the proper motions determined from the VLBI observations agree marginally

within the errors with the proper motions obtained with the Hipparcos satellite. The Hipparcos parallaxes for U Her and S CrB were quite uncertain, although they still agree with the VLBI parallaxes. Also the W Hya Hipparcos parallax agrees with our observations. The R Cas VLBI parallax is however, significantly smaller than found with Hipparcos. The Hipparcos parallaxes that were recalculated by Knapp et al. (2003) slightly improve the comparison for W Hya, S CrB and U Her, but the errors for S CrB and U Her remain large. The R Cas VLBI parallax remains significantly smaller.

It is important to realize that, because the stars in our sample are relatively faint variable AGB stars, some flags were attached to the Hipparcos catalogue entries regarding the processing of the astrometric data. The flags relevant to our comparison are listed in Table 4. The H29 flag gives the percentage of data that had to be rejected in order to obtain an acceptable astrometric solution. Both W Hya and S Crb had some data rejected, most likely due to observations at minimum light. The H30 flag indicates the goodness-of-fit (F2) of the astrometric solution. It is stated in the catalogue that fits with an F2 value exceeding +3 indicate a bad fit to the data. We immediately see that the Hipparcos result for W Hya is a very bad fit, while also the other 3 stars give only moderately acceptable fits. H59 is the flag indicating a possible double or multiple system, where "V" are labeled as "variability induced movers". This indicates that as a result of variability the data show additional motion. In itself this does not indicate bad astrometry, as it is simply a label given to many strongly variable stars. However, it does indicate that the reliability of the astrometric fit could be less. Finally an H61 flag "S" indicates a suspected non-single system when no significant or convincing non-single star solution is found. However, the catalogue suggests that many sources labeled "S" are actually single stars, with the flag induced by variability or
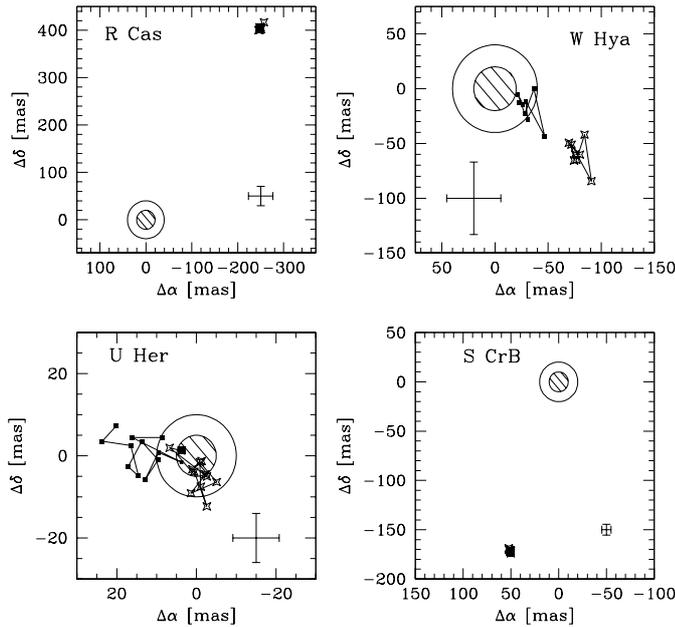
Fig. 10. The position of the observed maser spot wrt the optical position as predicted by our fits. The solid symbols denote the first epoch and subsequent epochs are connected. Also drawn are indications of the size of the star (shaded) and the radiophotosphere. The error bars in the corner are the errors due to the transposition of the radio positions and the Hipparcos position errors. The exact size of the error bars depends on the epoch of observations, the drawn error bars are for the middle epoch. For U Her and W Hya the squares indicate the transposed positions using the Hipparcos proper motion and parallax. Note the difference in scale of the four plots.

inadequate sampling. The flags are more thoroughly discussed in Perryman et al. (1997).

Because of these flags, the Hipparcos values, and especially the quoted errors should be treated with care. Especially for W Hya these can explain the differences between the Hipparcos and VLBI results.

The absolute astrometry of the observed maser spot positions can be compared with the Hipparcos optical position transposed from its mean observation epoch J1991.25 using the fitted proper motion. The errors in the comparison are due to the errors in the proper motion (and parallax) used to transpose the optical position to a common epoch. The alignment of the Hipparcos frame with the International Celestial Reference Frame (ICRF) was made at $\lesssim 1$ mas accuracy (Lestrade et al. 1995). The results are shown in Fig. 10. The U Her radiophotosphere was estimated have a diameter of ≈ 20 mas in vL00. W Hya was observed by Reid & Menten (1997) to have a radiophotosphere diameter of ≈ 80 mas at 22 GHz. From optical interferometry the diameter of R Cas was estimated to be ≈ 40 mas, giving a radiophotosphere of ≈ 80 mas if the radiophotosphere is twice the size of the star. For S CrB we have simply drawn an average size of 40 mas.

We find that the off-set between the maser and stellar positions is largest for the observed red-shifted maser spots of R Cas and S CrB. While the error of the transposed positions is ≈ 34 mas due to the extrapolation to a common epoch, we find a weighted average off-set of 474.2 mas with an rms

scatter of 3.6 mas for the maser of R Cas. At the assumed distance of R Cas this corresponds to ≈ 83 AU. For S CrB we find a weighted average off-set of 178.5 mas with an rms scatter of 1.2 mas, while the error due to the transposed positions is ≈ 7 mas. This off-set corresponds to ≈ 77 AU at 433 pc.

For the most blue-shifted maser spots of U Her we found in vL00, that the position matches the transposed Hipparcos optical position within the errors. With the improved parallax and proper motion fit we find a weighted average off-set of 4.1 ± 3.1 mas, corresponding to $\approx 1.1 \pm 0.8$ AU at the distance of U Her. With the errors of the transposition being ≈ 8 mas at the middle epoch, the most blue-shifted maser clearly falls onto the stellar radiophotosphere with a ≈ 10 mas radius. For a comparison, the Hipparcos optical position was also transposed using the Hipparcos values for proper motion and parallax. Using these the off-set increases to 13.0 ± 5.0 mas.

Although the fit of the motion of W Hya has large errors and left some unexplained residuals, a similar analysis was performed. Using our fitted motion, we find a weighted average off-set of 99.4 ± 9.4 mas, which would correspond to ≈ 9.7 AU. The errors due to the transposition were ≈ 42 mas due to the large error of the proper motion. We thus find that the most blue-shifted maser spot falls just outside the stellar radio-sphere with an assumed diameter of ≈ 80 mas. However, using the Hipparcos proper motion, the off-set decreases to 36.2 ± 11.6 mas, clearly on the stellar photosphere.

4. Discussion

4.1. Stellar motion and maser morphology

4.1.1. U Her

The masers of U Her were observed with respect to the reference source J1630+2131, which is located at $2.8°$ from U Her. The absolute astrometry was estimated to be accurate to ≈ 1.5 mas as determined from the relative reference source positions, but, as the reference sources have a smaller separation than their distance to U Her, the errors on U Her could be as large as 3 mas.

We managed to trace the most blue-shifted 1667 MHz OH maser spot of U Her for an additional 6 epochs, which combined with the observations in vL00 gives an improved fit of the proper motion and parallax of U Her. The proper motion in declination and the parallax are consistent with the results in vL00, but the proper motion in right ascension is somewhat smaller. Using the new values, the maser positions fall directly onto the transposed Hipparcos positions, without the seemingly systematic off-set detected in vL00. The separation between expected optical position and the radio position is only ≈ 1.1 AU and well within the diameter of the radiophotosphere. The rms residuals are consistent with the rather large target – reference source separation. This, together with possible turbulence of ≈ 0.7 mas/yr, can explain the residuals found in vL00 and observed here. As discussed above, the reference sources used to get the positions of the U Her maser spots shows some indication of source evolution, which was determined to possibly increase the measured proper motion by approximately 0.57
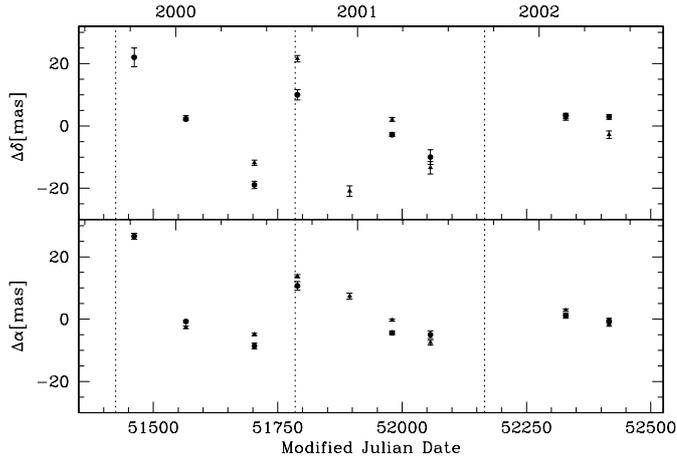
Fig. 11. The residual motion of the maser spots of W Hya after subtracting the best fitted model. The circles are the 1667 MHz spot and the triangles the 1665 MHz spot. The errors are the formal position fitting errors. The dashed vertical lines indicate the position of the maximum of the stellar phase.

and 0.10 mas/yr in right ascension and declination respectively. This does not affect the observed alignment of the maser positions with the optical position in Fig. 10, because the Hipparcos position, transposed using the fitted values, would experience the same positional shift as the maser positions.

In the course of the observations we did not find any other maser spots that were bright or persistent enough to trace its motion. The most blue-shifted spot was consistently the brightest, unlike in one of the epochs observed in vL00,

4.1.2. W Hya

The masers around the low declination source W Hya were observed with respect to the reference source J1342-290, located at 1.6° from W Hya. We were unable to establish a phase connection between the two reference sources themselves, but estimate the errors due to the ionosphere to be ≈4 mas.

Also for W Hya, we managed to trace the motion of the most blue-shifted maser feature. It was detected at both transitions, and the positions of the pair, matched to within ≈15 mas, approximately the size of the highly elongated beam. The best fitted model has large errors and it has been shown that also the Hipparcos results were labeled as a bad fit. Using the best fitted models we find that the maser spot position is off-set from the Hipparcos optical positions by almost 10 AU, however, when using the Hipparcos proper motion the maser spots are only off-set by ≈3.5 AU. Because the errors are large (≈4 AU), and the assumed radius of the radiophotosphere is ≈4 AU, we conclude that also for W Hya, the most blue-shifted maser spot is the amplified stellar image. The residuals from our fit, shown in Fig. 11 seem to describe some periodic fluctuations which are out of phase with the motion due to the parallax. The residual motions have a period between 300 and 400 days, and an amplitude of ≈15 mas which at the determined distance of W Hya corresponds to only ≈1.5 AU. At the assumed distance of W Hya (≈100 pc), a typical value of 1 km s^{-1} turbulent motion in the maser medium (Diamond et al. 1985) corresponds

to 2.1 mas/yr. Therefore, turbulence alone cannot explain the large residuals and it also seems unlikely that the phase referencing could introduce such large scatter. One possibility is that the stellar trajectory shows the effect of a binary or multiple system. However, this can be ruled out, as a motion of 15 mas and a period of approximately a year would indicate a companion of several solar masses within the stellar diameter. Another cause of the residuals could be stellar pulsations. There seems to be an indication that the residuals are correlated with the optical light curve. Because the compact maser spot is a result of strong beaming, the motions could result from minor changes in the maser medium due to a variation in pumping. Additionally, the maser spot can drift over the radiophotosphere due to intensity variations in the stellar radio emission, possibly caused by stellar pulsation. From optical measurements it has been shown that between optical minimum and maximum, the stellar diameter decreases by ≈20 mas (Lattanzi et al. 1997; Haniff et al. 1995). Lattanzi et al. (1997) have also shown that W Hya is highly elongated, with a major axis 20% larger than the minor axis. Consequently, the stellar pulsation can easily explain the large residuals observed.

4.1.3. R Cas

The masers around R Cas were observed with respect to the reference source J2355+495, at 1.6° from the star. The errors due to the ionosphere were estimated to be ≈3.6 mas.

The motion of R Cas was determined from a fit to the positions of a compact red-shifted maser spot at 1665 MHz. Since this spot is therefore not fixed to the stellar radiophotosphere we have to assume that the spot is stationary with respect to the star or on a linear path. A turbulent motion of 1 km s^{-1} at the distance of R Cas would result in additional motions of 1.5−2 mas/yr. Additionally, we can estimate the position shift we would observe due to a simple spherical outflow. We assume the transposed Hipparcos position to be the stellar position and the maser spot to be at 83 AU (Fig. 10), we take the expansion velocity to be 5.5 km s^{-1} and the OH maser extent to be ≈300 mas (Chapman et al. 1994). The maser spot would then move outward from the star at ≈2.5 mas/yr. This motion does not affect the parallax, but can explain the difference between the VLBI and Hipparcos proper motion. A parallax as large as the one found by Hipparcos does not fit our data and taking all errors into account we favor the VLBI parallax.

We can compare the location of the maser spot with respect to the star in Fig. 10, with the map of the 1665 and 1667 MHz OH masers features observed with MERLIN in Chapman et al. (1994). They found, as indicated in their Fig. 10, most of the red-shifted maser features to occur in a large region ≈400−600 mas from the most blue-shifted features. However, they observed the bright red-shifted features mainly in the 1665 MHz line and the bright blue-shifted features at 1667 MHz. The maps of the 1665 and 1667 MHz transitions were then aligned using the position of the centroids of the maser emission at the most blue-shifted and red-shifted velocity. As a result there could be a large error on the relative 1665 and 1667 maser positions. The position angle of the

red-shifted features with respect to the blue-shifted feature however, is the same as that of our bright maser spot with respect to the transposed stellar position. And since the separations are comparable it is likely that the stellar position coincides with the most blue-shifted features detected by Chapman et al. (1994). Although single dish spectra show that the red-shifted side of the spectrum is ≈2.5 times brighter than the blue-shifted side, it is somewhat surprising that no bright blue-shifted emission was detected in our observations. Either the stellar image is too faint to observe at VLBA baselines or the maser conditions changed between the epochs of observation (the MERLIN observations were performed in 1986). This is quite possible since the R Cas masers are found to be very a-spherical, possibly due to the presence of a companion star at 27.8 arcsec separation (Proust et al. 1981).

4.1.4. S CrB

The phase referencing of the S CrB masers was performed on reference source J1522+3144, at a separation of 0.4°. Because the source – reference source separation is so small, the errors due to the ionosphere are estimated to be less than 2.5 mas.

The motion of S CrB was also determined from observations of a red-shifted maser feature. This feature seems to correspond to the bright red-shifted maser emission observed in the single dish spectra of both main-line maser transitions (e.g. Fix 1978; Etoka et al. 2001). The brightest feature was detected in both transitions that coincide within ≈5 mas at each epoch, well within the beam size. However, this feature cannot be the stellar image. Since there are no published results on the morphology of the OH masers around S CrB we can only make a crude estimate on the systematic motion that might be present for the red-shifted maser spot. With an outflow velocity estimated from the single dish spectra of ≈4 km s^{-1} and a stellar velocity of 0.0 km s^{-1}, a red-shifted feature at a radial velocity of 3 km s^{-1} will have a transverse velocity of ≈2.6 km s^{-1}. At the distance of S CrB this would lead to a systematic motion of ≈1.3 mas/yr. Thus, a systematic error of ≈0.9 mas/yr could be present in the determined components of the proper motion. Turbulence could cause random motions of ≈0.5 mas/yr, while the phase referencing errors were estimated to be ≈2.5 mas. These errors however, were based on the separation between both of the reference sources, while the separation between S CrB and the reference source used for the calibration is much smaller. Thus, the residuals from our best fitted model (≈1.2 mas) are in excellent agreement with the phase referencing errors, and the maser spot does not seem to show any unexplained motions.

4.2. The nature of the brightest maser features

Whereas in U Her and W Hya the most blue-shifted maser spot is the amplified stellar image, both R Cas and S CrB did not show any compact blue-shifted maser spot. Instead we observed a compact red-shifted spot which could be traced for over 2 yrs. And even though it is not the amplified stellar image, the bright red-shifted maser feature of S CrB coincides in
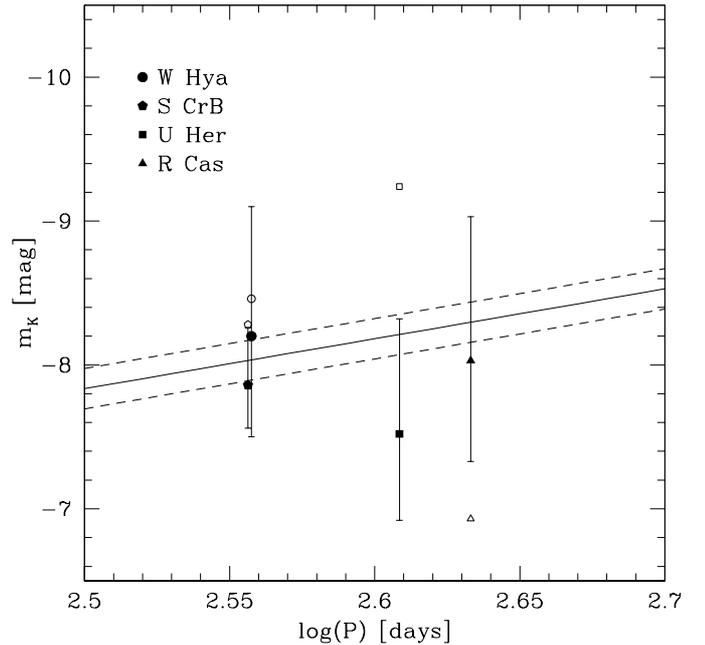

Fig. 12. Period vs. K_0 luminosity for the observed stars. The solid symbols and the error bars are determined using the distances obtained in this paper. The open symbols are the values using the Hipparcos distances. The solid line is the $P−L$ relation determined by Whitelock & Feast (2000) on the oxygen rich Mira stars observed with Hipparcos, the dashed lines are the spread in the relation due to the error in the $P−L$ relation zero-point.

the 1665 and 1667 MHz maser transition. Also, for both these stars the single dish maser spectra show stronger red-shifted emission than blue-shifted emission (e.g. Chapman et al. 1994; Etoka & Le Squeren 2000; Etoka et al. 2001).

As observed in one of the epochs of U Her discussed in vL00, features other than the most blue-shifted maser spot are occasionally dominant. This is likely caused by high density maser blobs or filaments, which can occur throughout the entire maser shell. Thus, these form of density enhancements can also explain the occurrence of compact red-shifted maser features.

In the case of R Cas, the observations of Chapman et al. (1994), do show some compact emission from the most blue-shifted side of the maser shell. According to the comparison with our observations this emission was likely the amplified stellar image. However, it was much weaker than the red-shifted emission and was not detected in our observations.

4.3. Distances

In Table 5 we compare the distances determined with VLBI monitoring of the OH maser spots with those determined with a $P−L$ relation. The table also lists the Hipparcos distance (including those as recalculated by Knapp et al. (2003), and the K_0 magnitude of our sources. The $P−L$ relation used to determine the values in the column labeled (2) is also shown in Fig. 12. We use the $P−L$ relation of the form

$$M_K = -3.47 \log P + \beta, \tag{1}$$

Table 5. Distances.

Source	K_0	Hipparcos	Hipparcos (1)	$P-L$ (2)	$P-L$ (3)	$P-L$ (4)	$P-L$ (5)	VLBI
	(mag)	(pc)	(pc)	(pc)	(pc)	(pc)	(pc)	(pc)
W Hya	−3.16	115	78	90	80	70	90	98^{+30}_{-18}
S CrB	0.32	526	417	470	410	340	450	433^{+72}_{-54}
U Her	−0.29	610	532	380	340	265	370	277^{+112}_{-62}
R Cas	−1.80	106	100	200	170	135	190	176^{+92}_{-45}

(1) Knapp et al. (2003), (2) Whitelock & Feast (2000), (3) Alvarez & Mennessier (1997),

(4) Bedding & Zijlstra (1998), (5) Chapman et al. (1994)

with the slope of the relation derived from Large Magellanic Cloud observation by Feast et al. (1989). The zero-point $\beta = 0.84 \pm 0.14$ was derived in Whitelock & Feast (2000) from a sample of 180 oxygen rich Miras from the Hipparcos catalogue. We see in Fig. 12 that the luminosities obtained with the VLBI distances show less scatter around the $P-L$ relation than the Hipparcos points.

The distances were also compared with the $P-L$ relation derived from the Hipparcos data by Alvarez & Mennessier (1997). They did not a priori assume a slope for the $P-L$ relation and divided their stellar sample into two groups based on the kinematics. For the first group, which is thought to mainly consist of late disk stars they found $M_K = -3.41 \log P + 0.976$. For the second group, thought to consist of stars that belong to an extended disk or to the halo, they found $M_K = -3.18 \log P - 0.129$. Based on their criteria it is likely that all our sources are from the first group. The distance values based on this relation are listed in the column labeled (3) of Table 5.

A third comparison was made with the $P-L$ relation found by Bedding & Zijlstra (1998) for Mira and Semiregular (SR) stars from the Hipparcos catalogue. They also did not fix the slope of the relation and found $M_K = -1.67 \log P - 3.05$. They used a sample of 6 Miras and 18 SR stars which had an Hipparcos parallax precision of $\sigma_\pi/\pi \leq 0.2$. The distance values based on this relation are listed in the column labeled (4) of Table 5.

It is of course possible, that since the Whitelock & Feast, Alvarez & Mennessier and Bedding & Zijlstra $P-L$ relations are all based on the Hipparcos data, a common bias could have been introduced. For comparison we have also used the relation from Chapman et al. (1994), which is given by Eq. (1) with $\beta = 0.93$. This is solely based on the LMC data of Feast et al. (1989), assuming a distance modulus to the LMC of 18.55. The resulting distances are shown in the column labeled (5) in Table 5.

The VLBI distances seem to agree best with the $P-L$ relations from Chapman et al. (1994) and Alvarez & Mennessier (1997) with only U Her being systematically fainter. As discussed in vL00, the size of U Her indicates that it pulsates in fundamental mode. R Cas is also thought to be a fundamental mode pulsator as shown in van Leeuwen (1997). This was determined by observations of the stellar radius, which seemed to be smaller than expected for overtone pulsators. However, our revised distance implies a larger radius, indicating that R Cas

is likely pulsating in an overtone. Because the other stars have periods less than 400 days they are also expected to be overtone pulsators. Since fundamental mode pulsators are somewhat fainter than predicted by the $P-L$ relation, this can explain the off-set observed for U Her.

4.4. Perspectives on maser astrometry

The previous result on U Her (vL00) indicated that one could follow the stellar trajectory accurately by VLBI monitoring the most compact blue-shifted emission in OH masers. The amplification of the stellar image would fulfill the requirement that an assumption has to be made that relates the maser motion to the stellar motion. In particular, to measure a parallax this tie must be much more accurate than 1 AU. From the small sample presented here, it has emerged that we cannot find such a special spot in every stellar OH maser. However, even without a stellar image, valid results can still be obtained from OH astrometry. For R Cas and S CrB we have successfully traced a bright maser spot in the shell that cannot be the amplified stellar image, as it originates from the far side of the expanding shell. The parallax can still be measured if we can assume that this maser spot has a constant relative motion with respect to the star. The proper motion of the star can only be obtained if the maser's peculiar motion can be assumed to be small or accurately known, for instance from the geometry of the shell. Our results indicate that the maser's motion with respect to the star is indeed small. Also, it is clear that these maser spots are persistent on the timescale of a few years.

The accuracy of the current measurements is limited by the ionosphere and the extrapolation of the calibrator phases. In principle, this restriction can be addressed by ionospheric calibration or by using closer (in-beam) position calibrators, as was shown for VLBI pulsar astrometry by Fomalont et al. (1999). However, for the OH masers, a 1 mas accuracy limitation seems to be intrinsic, as the maser spot brightness is relatively modest. A high precision parallax can be obtained by using many observation epochs and the proper motion can benefit from extending the time baseline, provided individual maser spots last long enough. At the OH maser frequency the technique is relatively straightforward, as the coherence time is long and calibrators are abundant. However, in this way, parallaxes can only be obtained for sources closer than 1 kpc. For SiO and H_2O masers the restrictions set by the limited brightness are lifted and stars

much further away could be probed. However, the coherence times are shorter and calibrators will be harder to find.

5. Conclusions

We have improved upon the distances and proper motions of U Her, S CrB and R Cas using VLBI astrometry of the 1665 and 1667 MHz OH masers. Also for the relatively close star W Hya we have fitted a stellar trajectory. However, large residuals remain in this fit and we attribute these to variations in the stellar photosphere which are important for a star as close as W Hya (Sect. 4.1.2). These variations introduce significant additional motions to a maser spot which is the amplified stellar image.

For U Her we traced the amplified stellar image, which we have now been able to follow for almost 8 yrs. For W Hya it is plausible that the bright maser spot is also the amplified stellar image. The other two stars do not show any blue maser spots that can be detected with VLBI, implying that the amplified stellar image is not dominant in all OH maser shells. Furthermore, it has been observed that the 1665 MHz and 1667 MHz masers can coincide on VLBI scales, even when they are not the amplified stellar image. Still, even the redshifted maser spots are shown to allow the determination of a good VLBI parallax and proper motion.

For phase referencing at 1.6 GHz the limitation in accuracy is the ionosphere, which is clearly demonstrated by the fact that the data quality steeply degrades near the maximum of solar activity. In all cases, but W Hya, the residuals in the data with respect to the best fit, can be entirely attributed to the ionosphere. Thus, there are no indications of additional motions in these stars, like, for instance, could be expected in binary systems.

We have shown that astrometry of OH maser spots with VLBI offers a unique possibility to measure the distances of enshrouded AGB stars. The four stars stars studied here are presumably losing mass more rapidly than the bulk of Mira variables, mostly studied with Hipparcos. Even so, we find these four stars now closely follow the established $P-L$ relation and fit the recent theories on pulsation modes.

References

Alvarez, R., & Mennessier, M.-O. 1997, A&A, 317, 761
Beasley, A. J., Gordon, D., Peck, A. B., et al. 2002, ApJS, 141, 13
Bedding, T. R., & Zijlstra, A. A. 1998, ApJ, 506, L47
Chapman, J. M, Sivagnanam, P., Cohen, R. J., & Le Squeren, A. M 1994, MNRAS, 268, 475
Diamond, P. J., Norris, R. P., Rowland, P. R., et al. 1985, MNRAS, 212, 1
Etoka, S., & Le Squeren, A. M. 2000, A&AS, 146, 179
Etoka, S., Blaszkiewicz, L., Szymczak, M., & Le Squeren, A. M. 2001, A&A, 378, 522
Feast, M. W., Glass, I. S., Whitelock, P. A., & Catchpole, R. M. 1989, MNRAS, 241, 375
Fix, J. D. 1978, ApJ, 223L, 25
Fomalont, E. B., Goss, W. M., Beasley, A. J., & Chatterjee, S. 1999, AJ, 117, 3025
Haniff, C. A., Scholz, M., & Tuthill, P. G. 1995, MNRAS, 276, 640
Knapp, G. R., Pourbaix, D., Platais, I., & Jorissen, A. 2003, [astro-ph/0301579]
Lattanzi, M. G., Munari, U., Whitelock, P. A., & Feast, M. W. 1997, ApJ, 485, 328
Lestrade, J.-F., Jones, D. L., Preston, R. A., et al. 1995, A&A, 304, 182
Norris, R. P., Booth, R. S., Diamond, P. J., et al. 1984, MNRAS, 208, 435
Perryman, M. A. C., Lindegren, L., Kovalevsky, J., et al. 1997, A&A, 323L, 49
Proust, D., Ochsenbein, F., & Pettersen, B. 1981, A&AS, 44, 179
Reid, M. J., & Menten, K. M. 1997, ApJ, 476, 327
Sivagnanam, P., Diamond, P. J., Le Squeren, A. M., & Biraud, F. 1990, A&A, 229, 171
Szymczak, M., Cohen, R. J., & Richards, A. M. S. 1998, MNRAS, 297, 1151
van Langevelde, H. J., Vlemmings, W., Diamond, P. J., et al. 2000, A&A, 357, 945 (vL00)
van Leeuwen, F., Feast, M. W., Whitelock, P. A., & Yudin, B. 1997, MNRAS, 287, 955
Vlemmings, W. H. T., van Langevelde, H. J., & Diamond, P. J. 2002, A&A, 393, L33
Whitelock, P., & Feast, M. 2000, MNRAS, 319, 759
Wood P. R. 1998, IAU Symp. 189, ed. T. R. Bedding, A. J. Booth & J. Davis (Dordrecht: Kluwer), 299